

Multi-kV class β -Ga₂O₃ MESFETs with a Lateral Figure of Merit up to 355 MW/cm²

Arkka Bhattacharyya^{*1}, Praneeth Ranga¹, Saurav Roy¹, Carl Peterson¹, Fikadu Alema²,
George Seryogin², Andrei Osinsky², Sriram Krishnamoorthy¹

¹Electrical and Computer Engineering, University of Utah, Salt Lake City 84112, USA

²Agnitron Technology Incorporated, Chanhassen, Minnesota 55317, USA

Email: a.bhattacharyya@utah.edu, sriram.krishnamoorthy@utah.edu

Abstract—We demonstrate over 3 kV gate-pad-connected field plated (GPFP) β -Ga₂O₃ lateral MESFETs with high lateral figure of merit (LFOM) using metalorganic vapor phase epitaxy (MOVPE) grown channel layers and regrown ohmic contact layers. Contact resistance (R_c) as low as 1.4 Ω .mm is achieved using an improved low-temperature MOVPE selective area regrowth process. The GPFP design adopted here using PECVD deposited SiN_x dielectric and SiN_x/SiO₂ wrap-around passivation exhibits up to ~14% improved R_{on} , up to ~70% improved breakdown voltage (V_{BR}) resulting up to over 3 \times higher LFOM compared to non-FP β -Ga₂O₃ lateral MESFETs. The V_{BR} (~2.5 kV) and LFOM (355 MW/cm²) measured simultaneously in our GPFP β -Ga₂O₃ lateral MESFET (with $L_{GD} = 10 \mu\text{m}$) is the highest value achieved in any depletion-mode β -Ga₂O₃ lateral device.

Index Terms—Ga₂O₃, MESFETs, MOVPE, regrown contacts, breakdown, kilovolt, lateral figure of merit, passivation, field plates.

I. INTRODUCTION

Over the last few years, the rapid advances in β -Ga₂O₃-based device performance has made it an attractive ultra-wide bandgap semiconductor for high power electronics mainly because of its intrinsic high projected breakdown field (~8 MV/cm) and the availability of high-quality melt-grown bulk substrates [1]–[6]. The device performance has rapidly progressed in both lateral and vertical geometries thanks to the simultaneous progress in high-quality epilayer growth technologies that includes mainly MBE, MOVPE and HVPE as well as device processing techniques [7]–[14]. Of all these epitaxial growth techniques, MOVPE has captivated widespread attention due to its versatility and ability to grow comparatively higher-quality epilayers that enables high room-temperature electron mobility values (close to the theoretical limit) and could be promising for fabricating Ga₂O₃ lateral FETs with high current densities as well as high breakdown voltages [10], [15]–[17].

Many new field management techniques have been successfully demonstrated in lateral β -Ga₂O₃-based devices that enabled high-breakdown voltages, high average breakdown fields, and high ($V_{BR}^2/R_{on,sp}$) lateral figure of merit but not simultaneously in the same device [3], [11], [18]. In other words, $V_{BR} > 2\text{kV}$, lateral $V_{BR}^2/R_{on,sp} > 300\text{MW/cm}^2$, and $E_{BR,AVG} > 2\text{MV/cm}$ could not be achieved simultaneously in the same device. This could be due to a combination of factors such as device design, device processing techniques (bulk or surface leakage paths) and more importantly the epilayer material quality. In this work, we address these issues using a gate-pad connected field plate (GPFP) design using a PECVD deposited SiN_x dielectric in a β -Ga₂O₃ MESFET with MOVPE-grown channel and contact layers.

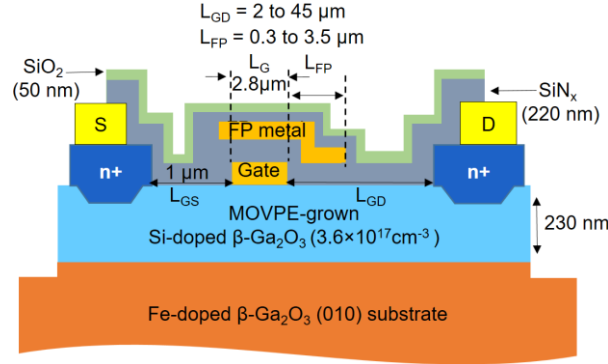


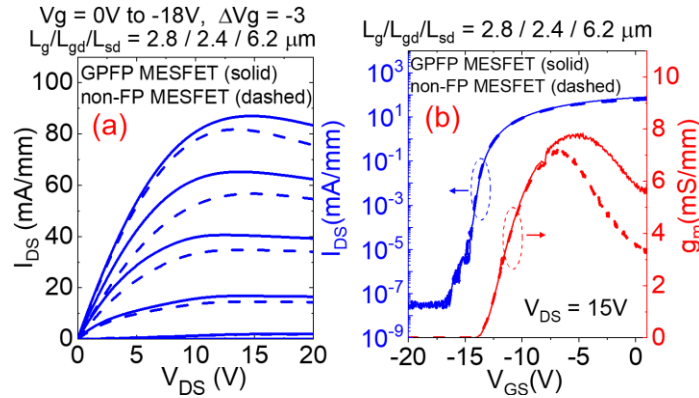
Fig. 1. Schematic of the GPFP β -Ga₂O₃ MESFET with a SiN_x/SiO₂ wrap-around passivation. The FP metal is electrically connected to the gate pad outside the mesa (not shown).

II. DEVICE GROWTH AND FABRICATION

The epitaxial structure shown in Fig. 1(a) consists of a β -Ga₂O₃ channel (230 nm thick Si-doped $\sim 3.6 \times 10^{17} \text{ cm}^{-3}$) on a Fe-doped (010) bulk substrates grown using Agnitron Technology's Agilis 700 MOVPE reactor with TEGa, O₂, and silane (SiH₄) as precursors and argon as carrier gas. Before the channel layer growth, the substrate was clean using HF for 30 mins. From Hall measurement, the channel charge and mobility were measured to be $5.7 \times 10^{12} \text{ cm}^{-2}$ and $95 \text{ cm}^2/\text{Vs}$ respectively, yielding a channel sheet resistance $R_{\text{sh, ch}} = 11.7 \text{ k}\Omega/\square$. The device mesa isolation and the source/drain ohmic contacts were selectively regrown by MOVPE technique using a Ni/SiO₂ mask pattern [19]. The contact recess etch was performed using a low power SF₆/Ar ICP-RIE dry etching, followed by a quick dip in a diluted BOE solution. The etching in the contact regions was extended down to the Ga₂O₃ epitaxial layer with an estimated Ga₂O₃ trench depths of 10-20 nm (Ga₂O₃ etch rate $\sim 1.5 \text{ nm/min}$). The Si-doping in the regrown n+ layer was $\sim 2.6 \times 10^{20} \text{ cm}^{-3}$. Following the contact regrowth process, ohmic metal stack Ti/Au/Ni (20 nm/100 nm/30 nm) was evaporated on the regrown contact regions using photolithography patterning and lift off, followed by a 450°C anneal in N₂ for 1.5 mins. Ni/Au/Ni (30 nm/100 nm/30 nm) metal stack was then evaporated to form the Schottky gate for the MESFET structure.

The gate field plate design used in this work is shown in Fig.1, where the gate field plate metal was electrically connected to the gate pad (shorted) outside the device mesa, hence, named gate-pad-connected field plate (GPFP). This design was adopted to protect the channel region from the dry-etching plasma damage that occurs in the conventional gate field plate etch process flow. The gate field plate metal was deposited following a SiN_x (170 nm thick) passivation layer deposited using PECVD (at 300°C). The field plate extension (L_{FP}) was varied from ~ 0.3 to $3.5 \mu\text{m}$ as the gate-to-drain distance (L_{GD}) varied from 2 to $45 \mu\text{m}$. Finally, the whole active region was passivated using a SiN_x/SiO₂ (50 nm/50 nm) bilayer dielectric deposited using the same PECVD (300°C) technique.

III. RESULTS AND DISCUSSIONS



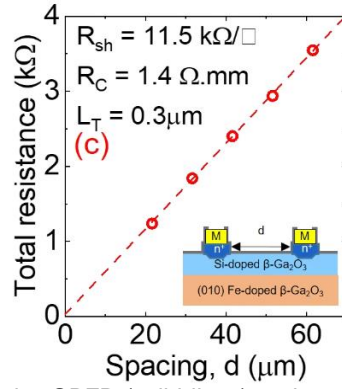


Fig. 2. (a) Output and (b) transfer curves for the GPFP (solid lines) and non-FP (dashed lines) β -Ga₂O₃ MESFETs. (c) Total resistance vs spacing for the TLM patterns (schematic shown in inset).

Fig. 2(a) & 2(b) show the DC output and transfer curves for the GPFP MESFET (solid lines) and the unpassivated non-FP MESFET (dashed lines) for device with dimensions $L_{GS}/L_G/L_{GD} = 1.0/2.8/2.4 \mu\text{m}$. No hysteresis was observed in the DC current-voltage dual sweeps. The $I_{DS,MAX}$ (for $V_{GS} = 0\text{V}$) measured was 88 mA/mm for the passivated GPFP MESFET and 81 mA/mm for the un-passivated non-FP MESFET. The ON resistance (R_{ON}) extracted from the linear region of the output curves were found to be 55.8 $\Omega\cdot\text{mm}$ for the GPFP MESFET and 63.2 $\Omega\cdot\text{mm}$ for the non-FP MESFET. From TLM measurements, the total R_C (contact resistance) measured was 1.4 $\Omega\cdot\text{mm}$ ($< 3\%$ of the total device R_{ON}) as shown in Fig. 2(c). Compared to our previous work, the ten-fold improvement in R_C was achieved using a slow etch rate SF_6/Ar dry etching [19]. The transfer curves show that both devices have low leakage ($\sim 10^{-12}$ A/mm) and high I_{ON}/I_{OFF} ratio $\sim 10^{10}$. The passivated GPFP MESFETs show $\sim 14\%$ lower R_{ON} , $\sim 8\%$ higher ON currents, and $\sim 13\%$ higher transconductance compared to the non-FP MESFETs clearly indicating the FP design used here not only preserves the R_{ON} in these devices, rather improves it possibly due to reduction of upward surface band-bending in the open access regions due to the SiN_x passivation [20].

Fig. 3(a) shows the three-terminal breakdown characteristics (at $V_{GS} = -20\text{V}$) of the non-FP MESFETs and the GPFP MESFETs with various L_{GD} values. All the breakdown measurements were performed with the wafer submerged in FC-40 Fluorinert dielectric liquid. Comparing devices with identical L_{GD} values, the GPFP MESFETs show significant improvement in breakdown voltage ($V_{BR} = V_{DS} - V_{GS}$) over the non-FP MESFETs. The highest measurable V_{BR} recorded was 2462V ($L_{GD}=10\mu\text{m}$) for the GPFP MESFET, which is $\sim 70\%$ higher compared to the non-FP MESFET (1462V) of the same dimension showing the efficacy of the FP design demonstrated here.

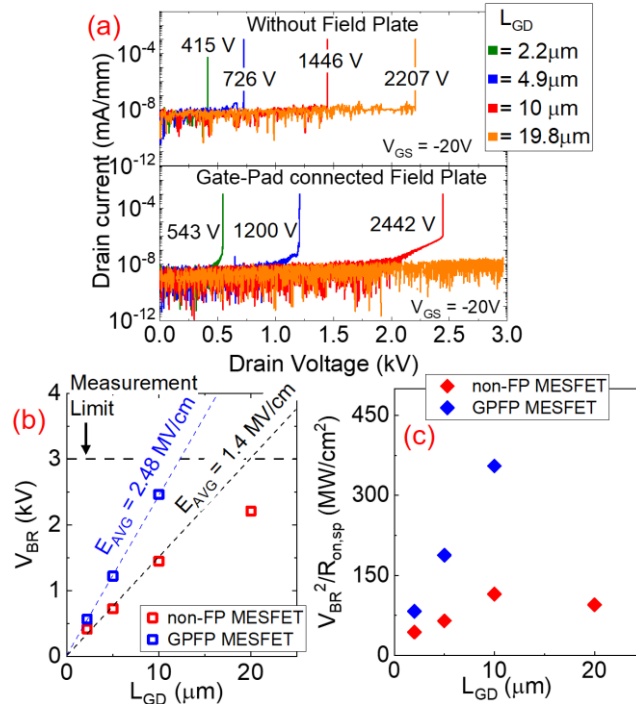


Fig. 3. (a) Breakdown characteristics of the non-FP (top) and GPFP (bottom) β -Ga₂O₃ MESFETs with various L_{GD} values. (b) V_{BR} as a function of L_{GD} for the non-FP and GPFP MESFETs showing the increase in $E_{BR,AVG}$, and improved V_{BR} vs L_{GD} linearity. (c) LFOM of the MESFETs as a function of L_{GD} .

It can be seen that for the GPFP MESFET, the V_{BR} scales more linearly with L_{GD} compared to the non-FP MESFETs (Fig.3(b)). Even though the E-field profile is highly non-uniform in the gate-drain region of a lateral device, an effective average lateral field ($E_{AVG} = V_{BR}/L_{GD}$) can be defined to be used as a metric to understand the scaling of breakdown voltage vs spacing and helps with lateral device design. Given that the field peaking around contact edges scales non-linearly and the transition from punch-through to non punch-through field profile with higher L_{GD} , the V_{BR} vs L_{GD} can be expected to be non-linear (the $E_{BR,AVG}$ can reduce). However, the calculated E_{AVG} values remained uniform ~ 2.5 MV/cm for GPFP MESFETs with L_{GD} up to 10 μm . This combination of E_{AVG} (~ 2.5 MV/cm) and V_{BR} (~ 2.5 kV) demonstrated here for a MESFET with $L_{GD} = 10$ μm is the highest till date for any depletion-mode Ga₂O₃ lateral device. GPFP MESFETs with L_{GD} 20 μm and above were measured repeatedly up to 3 kV (our measurement tool limit) without showing any degradation, demonstrating the robustness of these devices to high voltage stresses. It should be noted that all the devices in this work exhibit catastrophic breakdown.

To understand the electric field profiles, the device structure was simulated using Sentaurus TCAD under the breakdown condition ($L_{GD} = 10$ μm). The E_{peak} was found to be at the FP edge as expected (Fig. 4(b)). The sharp metal edges used in the simulation act as points of singularity in the Poisson solver and may overestimate actual peak field values in real devices. The electric field under the gate was found to be < 2 MV/cm, but the E_{peak} values in the SiN_x at the FP edge were found to be much higher (1.4 – 1.8 \times higher) than in Ga₂O₃. Therefore, it is possible that the dielectric breakdown was the dominant mechanism for large L_{GD} values rather than just the gate (tunneling) leakage.

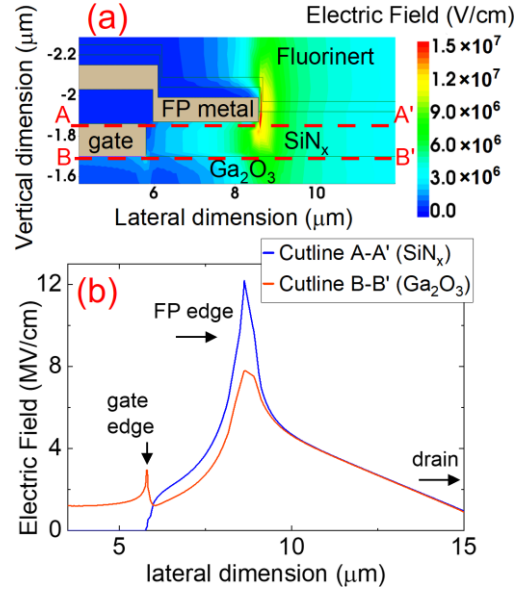


Fig. 4 (a) Simulated 2D electric field contour for a device with $L_{GD} = 10$ μm at the experimental breakdown condition of $V_{DG} = 2462\text{V}$. (b) E-Field profile inside the SiN_x and Ga₂O₃ along cutlines A-A' and B-B' resp. as shown in (a).

The lateral figures of merit ($V_{BR}^2/R_{on,sp}$) of the GPFP MESFETs were calculated, where $R_{on,sp}$ is R_{ON} normalized to the device length ($L_{SD} + 2L_T$). The LFOM values for the GPFP and non-FP MESFETs are plotted as a function of L_{GD} (Fig.3(c)). The highest LFOM of 355 MW/cm² was calculated for GPFP MESFET with an L_{GD} of 10 μm which is more than 3 \times higher than the non-FP MESFET (115 MW/cm²). Overall, the GPFP design is found to have 2-3 times higher LFOM compared to the non-FP design. This is because of the improved $R_{on,sp}$ (up to 14% lower) and V_{BR} (up to 70% higher) values simultaneously with the GPFP design. Given the GPFP MESFET with $L_{GD}=20\mu\text{m}$ have $V_{BR} > 3$ kV, the devices can demonstrate LFOM > 200 MW/cm². Fig. 5 benchmarks our $V_{BR}^2-R_{on,sp}$ values with the existing literature reports showing that the reported GPFP β -Ga₂O₃ MESFET shows the highest LFOM for $V_{BR} > 2$ kV, outperforming the likes of Ga₂O₃ MOSFETs and even advanced device designs like (AlGa)₂O₃/Ga₂O₃ HFETs and NiO_x/Ga₂O₃ p-n hetero-Junction FETs (hJFETs) [3], [18]. With the implementation of a gate dielectric, we expect the

LFOM values could be further improved provided gate dielectrics with low-leakage, cleaner interface and more importantly, dielectrics with high breakdown fields could be deposited along with high-quality β -Ga₂O₃ epitaxial layers.

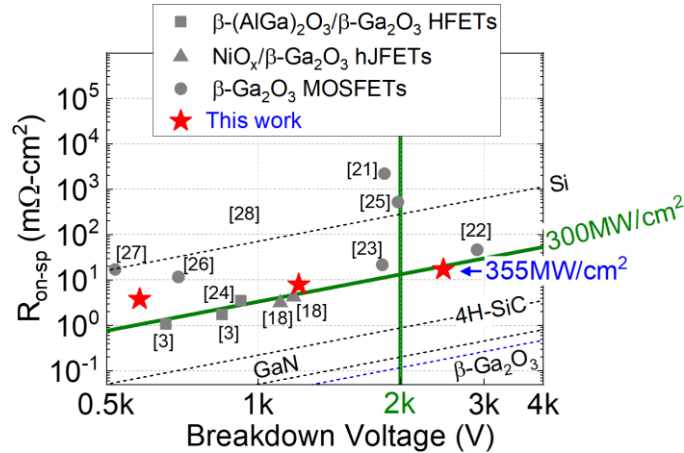


Fig. 5: Differential $R_{on,sp}$ - V_{BR} benchmark plot of our β -Ga₂O₃ MESFETs with the literature reports [3], [18], [21]–[27].

IV. CONCLUSION

We demonstrate gate-pad connected field plated MOVPE-grown kV-class β -Ga₂O₃ lateral MESFETs with high LFOM and $E_{BR,AVG}$ using PECVD deposited SiN_x and SiO₂ field/passivation dielectrics. A record high LFOM of 355 MW/cm² with a V_{BR} of ~2.5 kV and E_{AVG} of ~2.5 MV/cm simultaneously is demonstrated in a GPFP β -Ga₂O₃ MESFET with (L_{GD} =10 μ m). This LFOM value is the highest for any β -Ga₂O₃ lateral device with $V_{BR} > 2$ kV. These devices show great potential of MOVPE-grown β -Ga₂O₃ FETs for future power device applications in the low to medium voltage range.

V. ACKNOWLEDGEMENT

This material is based upon work supported by the II-VI foundation Block Gift Program 2020-2021 and the DoD SBIR Phase I – AF203-CS01 (Contract #: FA864921P0304).

REFERENCES

- [1] M. Higashiwaki and G. H. Jessen, "Guest Editorial: The dawn of gallium oxide microelectronics," *Appl. Phys. Lett.*, vol. 112, no. 6, p. 060401, Feb. 2018, doi: 10.1063/1.5017845.
- [2] "A review of Ga₂O₃ materials, processing, and devices: Applied Physics Reviews: Vol 5, No 1." <https://aip.scitation.org/doi/abs/10.1063/1.5006941> (2021).
- [3] N. K. Kalarickal *et al.*, " β -(Al_{0.18}Ga_{0.82})₂O₃/Ga₂O₃ Double Heterojunction Transistor with Average Field of 5.5 MV/cm," *IEEE Electron Device Letters*, pp. 1–1, 2021, doi: 10.1109/LED.2021.3072052.
- [4] S. Roy, A. Bhattacharyya, P. Ranga, H. Splawn, J. Leach, and S. Krishnamoorthy, "High Permittivity Dielectric Field-Plated Vertical (001) β -Ga₂O₃ Schottky Barrier Diode with Surface Breakdown Electric Field of 5.45 MV/cm and BFOM of > 1 GW/cm²," *arXiv:2105.04413 [cond-mat, physics:physics]*, May 2021, Accessed: May 18, 2021. [Online]. Available: <http://arxiv.org/abs/2105.04413>
- [5] A. J. Green *et al.*, "3.8-MV/cm Breakdown Strength of MOVPE-Grown Sn-Doped β -Ga₂O₃ MOSFETs," *IEEE Electron Device Letters*, vol. 37, no. 7, pp. 902–905, Jul. 2016, doi: 10.1109/LED.2016.2568139.
- [6] W. Li, K. Nomoto, Z. Hu, D. Jena, and H. G. Xing, "Field-Plated Ga₂O₃ Trench Schottky Barrier Diodes With a $BV^2/R_{on,sp}$ of up to 0.95 GW/cm²," *IEEE Electron Device Letters*, vol. 41, no. 1, pp. 107–110, Jan. 2020, doi: 10.1109/LED.2019.2953559.
- [7] P. Ranga *et al.*, "Delta-doped β -Ga₂O₃ thin films and β -(Al_{0.26}Ga_{0.74})₂O₃/ β -Ga₂O₃ heterostructures grown by metalorganic vapor-phase epitaxy," *Appl. Phys. Express*, vol. 12, no. 11, p. 111004, Nov. 2019, doi: 10.7567/1882-0786/ab47b8.
- [8] P. Ranga, A. Bhattacharyya, A. Chmielewski, S. Roy, N. Alem, and S. Krishnamoorthy, "Delta-doped β -Ga₂O₃ films with narrow FWHM grown by metalorganic vapor-phase epitaxy," *Appl. Phys. Lett.*, vol. 117, no. 17, p. 172105, Oct. 2020, doi: 10.1063/5.0027827.
- [9] P. Ranga *et al.*, "Growth and characterization of metalorganic vapor-phase epitaxy-grown β -(Al_xGa_{1-x})₂O₃/ β -Ga₂O₃ heterostructure channels," *Appl. Phys. Express*, vol. 14, no. 2, p. 025501, Jan. 2021, doi: 10.35848/1882-0786/abd675.

- [10] Z. Feng, A. F. M. Anhar Uddin Bhuiyan, M. R. Karim, and H. Zhao, "MOCVD homoepitaxy of Si-doped (010) β -Ga₂O₃ thin films with superior transport properties," *Appl. Phys. Lett.*, vol. 114, no. 25, p. 250601, Jun. 2019, doi: 10.1063/1.5109678.
- [11] S. Sharma, K. Zeng, S. Saha, and U. Singiseti, "Field-Plated Lateral Ga₂O₃ MOSFETs With Polymer Passivation and 8.03 kV Breakdown Voltage," *IEEE Electron Device Letters*, vol. 41, no. 6, pp. 836–839, Jun. 2020, doi: 10.1109/LED.2020.2991146.
- [12] S. Bin Anooz *et al.*, "Step flow growth of β -Ga₂O₃ thin films on vicinal (100) β -Ga₂O₃ substrates grown by MOVPE," *Appl. Phys. Lett.*, vol. 116, no. 18, p. 182106, May 2020, doi: 10.1063/5.0005403.
- [13] J. H. Leach, K. Udway, J. Rumsey, G. Dodson, H. Splawn, and K. R. Evans, "Halide vapor phase epitaxial growth of β -Ga₂O₃ and α -Ga₂O₃ films," *APL Materials*, vol. 7, no. 2, p. 022504, Feb. 2019, doi: 10.1063/1.5055680.
- [14] H. Murakami *et al.*, "Homoepitaxial growth of β -Ga₂O₃ layers by halide vapor phase epitaxy," *Appl. Phys. Express*, vol. 8, no. 1, p. 015503, Dec. 2014, doi: 10.7567/APEX.8.015503.
- [15] A. Bhattacharyya, P. Ranga, S. Roy, J. Ogle, L. Whittaker-Brooks, and S. Krishnamoorthy, "Low temperature homoepitaxy of (010) β -Ga₂O₃ by metalorganic vapor phase epitaxy: Expanding the growth window," *Appl. Phys. Lett.*, vol. 117, no. 14, p. 142102, Oct. 2020, doi: 10.1063/5.0023778.
- [16] Y. Zhang *et al.*, "MOCVD grown epitaxial β -Ga₂O₃ thin film with an electron mobility of 176 cm²/Vs at room temperature," *APL Materials*, vol. 7, no. 2, p. 022506, Dec. 2018, doi: 10.1063/1.5058059.
- [17] G. Seryogin *et al.*, "MOCVD growth of high purity Ga₂O₃ epitaxial films using trimethylgallium precursor," *Appl. Phys. Lett.*, vol. 117, no. 26, p. 262101, Dec. 2020, doi: 10.1063/5.0031484.
- [18] C. Wang *et al.*, "Demonstration of the p-NiOx/n-Ga₂O₃ Heterojunction Gate FETs and Diodes With BV²/R_{on,sp} Figures of Merit of 0.39 GW/cm² and 1.38 GW/cm²," *IEEE Electron Device Letters*, vol. 42, no. 4, pp. 485–488, Apr. 2021, doi: 10.1109/LED.2021.3062851.
- [19] A. Bhattacharyya *et al.*, "130 mA/mm β -Ga₂O₃ metal semiconductor field effect transistor with low-temperature metalorganic vapor phase epitaxy-regrown ohmic contacts," *Appl. Phys. Express*, 2021, doi: 10.35848/1882-0786/ac07ef.
- [20] C. Joishi *et al.*, "Breakdown Characteristics of β -(Al_{0.22}Ga_{0.78})₂O₃/Ga₂O₃ Field-Plated Modulation-Doped Field-Effect Transistors," *IEEE Electron Device Letters*, vol. 40, no. 8, pp. 1241–1244, Aug. 2019, doi: 10.1109/LED.2019.2921116.
- [21] K. Zeng, A. Vaidya, and U. Singiseti, "1.85 kV Breakdown Voltage in Lateral Field-Plated Ga₂O₃ MOSFETs," *IEEE Electron Device Letters*, vol. 39, no. 9, pp. 1385–1388, Sep. 2018, doi: 10.1109/LED.2018.2859049.
- [22] Y. Lv *et al.*, "Lateral β -Ga₂O₃ MOSFETs With High Power Figure of Merit of 277 MW/cm²," *IEEE Electron Device Letters*, vol. 41, no. 4, pp. 537–540, Apr. 2020, doi: 10.1109/LED.2020.2974515.
- [23] K. Tetzner *et al.*, "Lateral 1.8 kV β -Ga₂O₃ MOSFET With 155 MW/cm² Power Figure of Merit," *IEEE Electron Device Letters*, vol. 40, no. 9, pp. 1503–1506, Sep. 2019, doi: 10.1109/LED.2019.2930189.
- [24] N. K. Kalarickal *et al.*, "Electrostatic Engineering Using Extreme Permittivity Materials for Ultra-Wide Bandgap Semiconductor Transistors," *IEEE Transactions on Electron Devices*, vol. 68, no. 1, pp. 29–35, Jan. 2021, doi: 10.1109/TED.2020.3037271.
- [25] K. Zeng, A. Vaidya, and U. Singiseti, "A field-plated Ga₂O₃ MOSFET with near 2-kV breakdown voltage and 520 m Ω -cm²," *Appl. Phys. Express*, vol. 12, no. 8, p. 081003, Jul. 2019, doi: 10.7567/1882-0786/ab2e86.
- [26] Y. Lv *et al.*, "Source-Field-Plated β -Ga₂O₃ MOSFET With Record Power Figure of Merit of 50.4 MW/cm²," *IEEE Electron Device Letters*, vol. 40, no. 1, pp. 83–86, Jan. 2019, doi: 10.1109/LED.2018.2881274.
- [27] K. D. Chabak *et al.*, "Recessed-Gate Enhancement-Mode β -Ga₂O₃ MOSFETs," *IEEE Electron Device Letters*, vol. 39, no. 1, pp. 67–70, Jan. 2018, doi: 10.1109/LED.2017.2779867.